Journal of Organometallic Chemistry, 410 (1991) 211–229
Elsevier Sequoia S.A., Lausanne
JOM 21715

Cluster chemistry

LXVIII *. Substitution of CO by $P(OEt)_3$ in $Ru_5(\mu_5\text{-}C_2PPh_2)(\mu\text{-}PPh_2)(CO)_{13}$. X-Ray structures of two isomers of $Ru_5(\mu_5\text{-}C_2PPh_2)(\mu\text{-}PPh_2)(CO)_{12}\{P(OEt)_3\}$ and of $Ru_5(\mu_5\text{-}C_2PPh_2)(\mu\text{-}PPh_2)(CO)_{11}\{P(OEt)_3\}_2$

Michael I. Bruce, Michael J. Liddell, Edward R.T. Tiekink

Jordan Laboratories, Department of Physical and Inorganic Chemistry, University of Adelaide, Adelaide, South Australia 5001 (Australia)

Brian K. Nicholson

School of Chemistry, University of Waikato, Hamilton (New Zealand)

Brian W. Skelton and Allan H. White

Department of Physical and Inorganic Chemistry, University of Western Australia, Nedlands, Western Australia 6009 (Australia)

(Received December 20th, 1990)

Abstract

Reactions of $Ru_5(\mu_5\text{-}C_2PPh_2)(\mu\text{-}PPh_2)(CO)_{13}$ (**1**) with $P(OEt)_3$ occur preferentially at basal (thermal) or wing-tip Ru atoms (Me_3NO-induced); disubstitution gave a complex in which both phosphite ligands were on wing-tip Ru atoms, as did the reaction between **1** and PMe_2Ph. The X-ray structures of two isomers of the mono-substituted complex, containing $P(OEt)_3$ on wing-tip or basal Ru atoms, and of the disubstituted $P(OEt)_3$ complex were determined.

Introduction

The reaction between CO and the open pentanuclear cluster complex $Ru_5(\mu_5\text{-}\eta^2,P\text{-}C_2PPh_2)(\mu\text{-}PPh_2)(CO)_{13}$ (**1**; Scheme 1) [2] results in addition of two CO molecules with concomitant opening of two Ru–Ru bonds to form two isomers of the 'scorpion' cluster $Ru_5(\mu_5\text{-}C_2PPh_2)(CO)_{15}$ (**2k**, **2t**) [3]. We were also interested to determine the site of attack of nucleophiles such as tertiary phosphites or phos-

* For Part LXVII, see ref. 1.

0022-328X/91/$03.50

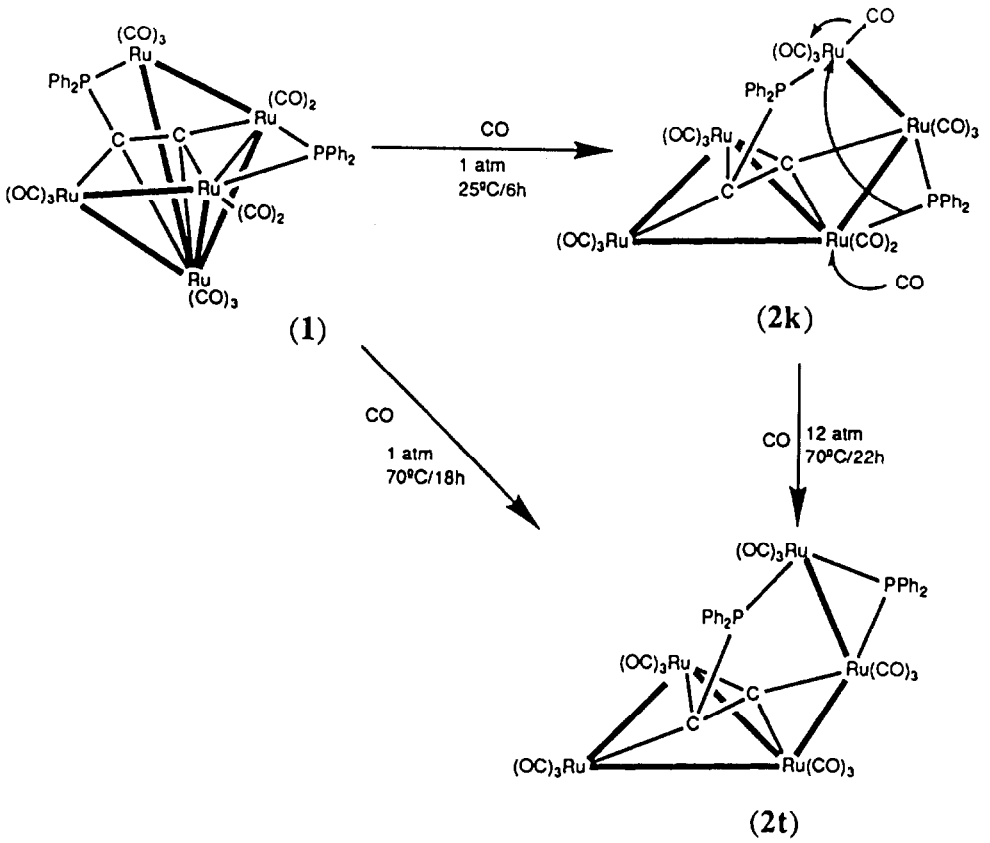

Scheme 1. Reactions of $Ru_5(\mu_5\text{-}C_2PPh_2)(\mu\text{-}PPh_2)(CO)_{13}$ (1) with CO.

phines, so we have examined the reactions of **1** with $P(OEt)_3$ and with PMe_2Ph. As described below, isomeric mixtures of products were obtained, and to help in the interpretation of these reactions, we have determined the molecular structures of the three title complexes.

Results

CO substitution by $P(OEt)_3$ in 1

Two routes to carbonyl substitution in **1** by $P(OEt)_3$ were investigated: (i) trimethylamine oxide-promoted, and (ii) thermally assisted. The first method involved treating an acetone solution of **1** with Me_3NO and $P(OEt)_3$ at 0 °C. The two products isolated from this reaction were found to be isomers of $Ru_5(\mu_5\text{-}C_2PPh_2)(\mu\text{-}PPh_2)(CO)_{12}\{P(OEt)_3\}$, **3a** and **3b** (Scheme 2). A third isomer of this complex, **3c**, was the major product isolated from the thermal reaction of **1** with $P(OEt)_3$ in cyclohexane at 45 °C. In the latter reaction, a disubstituted product $Ru_5(\mu_5\text{-}C_2PPh_2)(\mu\text{-}PPh_2)(CO)_{11}\{P(OEt)_3\}_2$ (**4**) was also formed, together with small amounts of **3a** and **3b**. When the thermal reaction was carried out in acetone, a lower yield of **3c** and a higher yield of **4** were obtained. A side product,

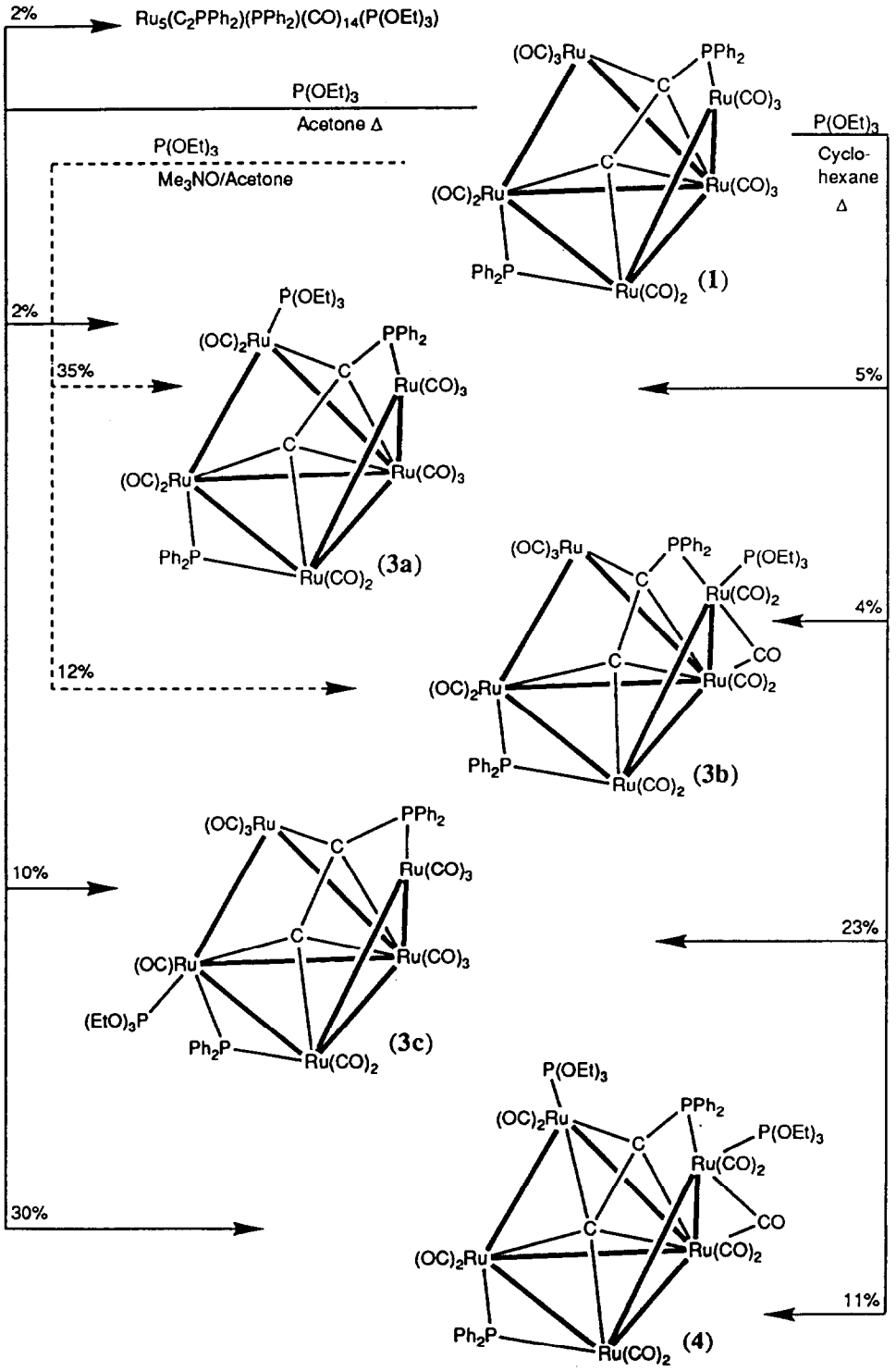

Scheme 2. Reactions of $Ru_5(\mu_5\text{-}C_2PPh_2)(\mu\text{-}PPh_2)(CO)_{13}$ (1) with $P(OEt)_3$.

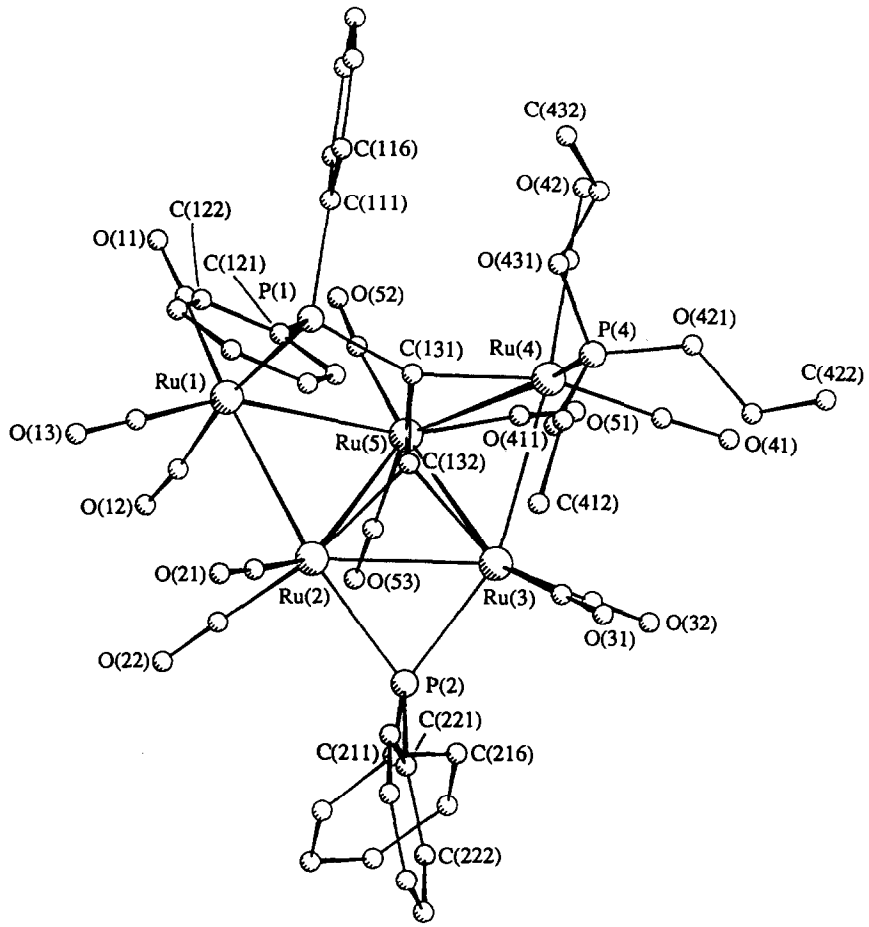

Fig. 1. Molecular structure and crystallographic numbering scheme for $Ru_5(\mu_5\text{-}C_2PPh_2)(\mu\text{-}PPh_2)(CO)_{12}\{P(OEt)_3\}$ (**3a**).

$Ru_5(\mu_5\text{-}C_2PPh_2)(\mu\text{-}PPh_2)(CO)_{14}\{P(OEt)_3\}$ obtained in this last reaction was apparently formed by ligand substitution of **2** (Scheme 1).

The four complexes **3a–3c** and **4** are dark brown crystalline solids, which were characterized in the first instance by spectroscopy and microanalysis and later by X-ray studies for **3a**, **3c** and **4**. The FAB mass spectra for these complexes showed molecular ions at m/z 1402 (monosubstituted) or at m/z 1542 (disubstituted), with ions formed by loss of the CO groups. Proton NMR spectra for the complexes exhibited signals between δ 8.1 and 7.2 for the phenyl groups and two multiplets for the alkyl protons. The low field CH_2 multiplets of the phosphite ligand(s) [δ 3.92 (**3a**); 4.03 (**3b**); 3.41 (**3c**); 3.92, 3.77 (P(3), P(4), respectively; see Fig. 3 below) (**4**)] were in some cases coupled to the phosphorus atom as well as to the CH_3 groups. A quintet was found for the CH_2 group in complexes **3a** and **3b**. Complex **3a** does not have a phosphido-group attached to the phosphite-bound ruthenium. The quintet, therefore, appears as a result of two overlapping quartets, and accords with each proton on the CH_2 group being slightly inequivalent. Of the two CH_2 signals found

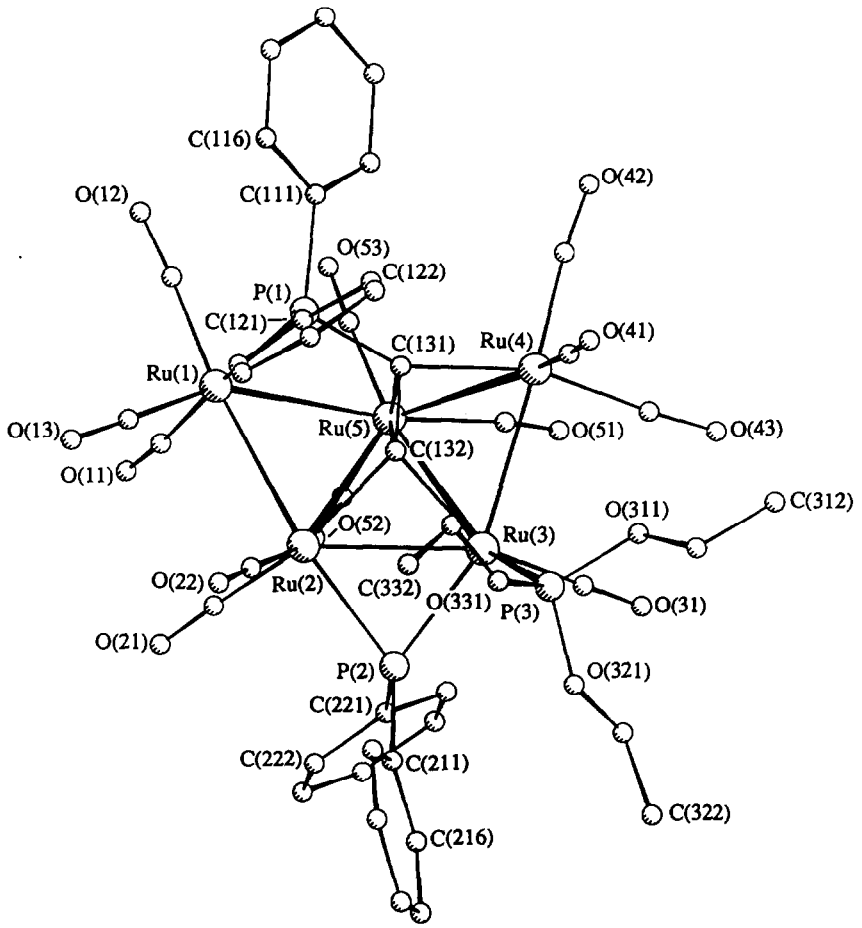

Fig. 2. Molecular structure and crystallographic numbering scheme for $Ru_5(\mu_5\text{-}C_2PPh_2)(\mu\text{-}PPh_2)(CO)_{12}\{P(OEt)_3\}$ (**3c**).

for **4**, the pseudo-quartet at δ 3.92 was assigned to P(3), as it showed coupling to P(1), and the quintet at δ 3.77 was assigned to P(4). The fourteen-line pattern at δ 3.41 in **3c** is a result of long range coupling. A detailed theoretical account of $X_nAA'X'_n$ coupling patterns has been given by Harris [4] for complexes containing two P-donor ligands at a metal centre. From this it is apparent that an $X_9X_6AA'X'_6Y'_9$ spin system would be very complex. For small $J_{AA'}$ the spectrum will tend towards the first-order spectrum, which for the CH_2 signal is a quartet (J(HH)) of doublets (J(PH)) of doublets (J(P'H)), as observed for complexes **3c** and **4**. The Me resonances are pseudo-triplets in each case.

X-ray crystallographic studies were carried out for complexes **3a**, **3c** and **4** to determine their molecular structures. Figures. 1–3 illustrate the three molecules, and Table 1 collects significant bond distances for these complexes and for complex **1**.

All four clusters have the same open metal framework, which comprises three edge-fused Ru_3 triangles. The monosubstituted complexes have the phosphite attached to either the wing-tip Ru(4) (in **3a**) or the basal Ru(3) (in **3c**), while in the

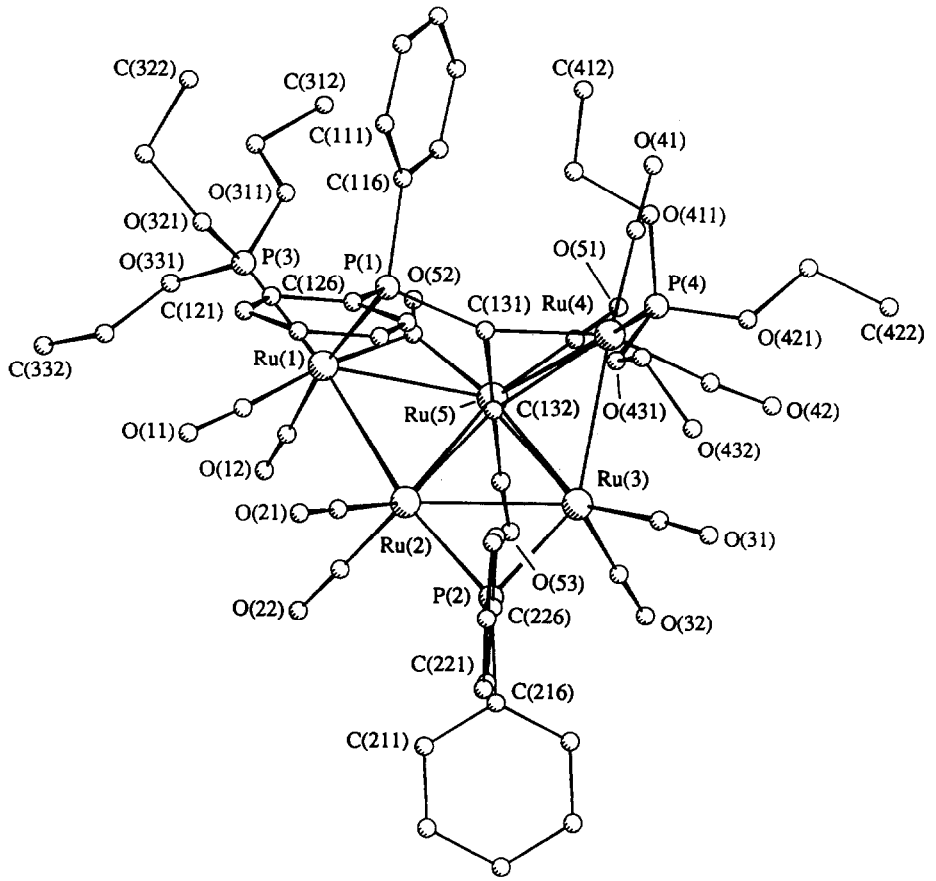

Fig. 3. Molecular structure and crystallographic numbering scheme for $Ru_5(\mu_5\text{-}C_2PPh_2)(\mu\text{-}PPh_2)(CO)_{11}\{P(OEt)_3\}_2$ (**4**).

bis-triethyl phosphite complex **4**, substitution at both wingtip rutheniums Ru(1) and Ru(4) has occurred. The relationships between these products is illustrated in Scheme 2. As can be seen from Table 1, the Ru–Ru bonds are in the ranges 2.754(1)–2.901(1) (**3a**), 2.747(1)–2.958(1) (**3c**) and 2.828(3)–3.009(2) Å (**4**). Addition of the phosphite ligands lengthens the metal–metal bonds slightly in complexes **3c** and **4** [$Ru\text{–}Ru_{av}$ 2.869 (**1**), 2.865 (**3a**), 2.877 (**3c**), 2.879 Å (**4**)]. The monosubstituted clusters have a shortest bond in common with **1**, viz. Ru(2)–Ru(3), the bond bridged by the phosphido group.

Compared with **1**, the *major* changes resulting from substitution of CO by $P(OEt)_3$ are confined to three of the Ru–Ru bonds. Thus, monosubstitution leads to a 0.03 Å contraction in Ru(1)–Ru(2); the increase in Ru(3)–Ru(5) in **3c** reflects the presence of the phosphite on Ru(3). Disubstitution results in lengthening of Ru(1)–Ru(2) by ca 0.07 Å, also a result of the steric influence of the phosphite at Ru(1). The pronounced lengthening of Ru(2)–Ru(3) in **4** is not so easily rationalised, but is concomitant with the changes in the swallow structure as may be seen by comparing the dihedral angles between the three Ru_3 planes in the four structures. In structures **1**, **3a**, **3c** and **4**, there is an opening of the Ru(1)–Ru(2)–Ru(3)–Ru(5)

Table 1

Significant bond distances (Å) and dihedral angles (deg) in complexes **1**, **3a**, **3c** and **4**

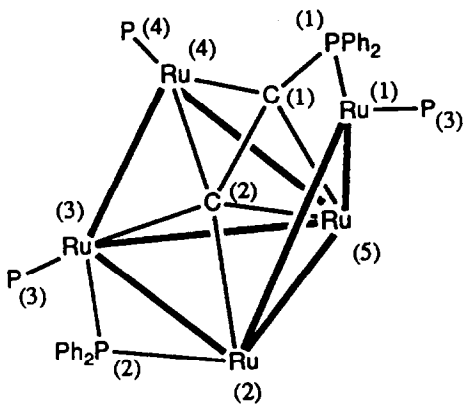

	1	3a	3c	4
Ru(1)–Ru(2)	2.932(2)	2.898(1)	2.894(1)	3.009(2)
Ru(1)–Ru(5)	2.921(2)	2.882(1)	2.932(1)	2.891(1)
Ru(2)–Ru(3)	2.731(2)	2.754(1)	2.747(1)	2.849(1)
Ru(2)–Ru(5)	2.890(1)	2.877(1)	2.882(1)	2.854(2)
Ru(3)–Ru(4)	2.854(2)	2.901(1)	2.872(1)	2.855(1)
Ru(3)–Ru(5)	2.909(1)	2.901(1)	2.958(1)	2.870(2)
Ru(4)–Ru(5)	2.848(1)	2.840(1)	2.857(1)	2.828(3)
Average	2.869	2.865	2.877	2.879
Ru(1)–P(1)	2.373(2)	2.369(2)	2.368(2)	2.391(6)
Ru(1)–P(3)				2.273(5)
Ru(2)–P(2)	2.353(2)	2.346(3)	2.351(3)	2.283(5)
Ru(3)–P(2)	2.279(2)	2.266(2)	2.271(2)	2.251(4)
Ru(3)–P(3)			2.220(2)	
Ru(4)–P(4)		2.242(2)		2.246(7)
Ru(2)–C(2)	2.016(5)	2.091(8)	2.081(8)	2.14(1)
Ru(3)–C(2)	2.024(5)	2.050(8)	2.051(9)	2.13(1)
Ru(4)–C(1)	2.055(5)	2.084(9)	2.089(8)	2.07(1)
Ru(4)–C(2)	2.586(5)		2.507(8)	2.33(1)
Ru(5)–C(1)	2.279(4)	2.323(6)	2.240(9)	2.30(1)
Ru(5)–C(2)	2.154(4)	2.184(7)	2.165(8)	2.22(3)
Dihedrals (deg)				
Ru(1)–Ru(2)–Ru(5)/ Ru(2)–Ru(3)–Ru(5)	152.4	158.3	154.4	166.3
Ru(2)–Ru(3)–Ru(5)/ Ru(3)–Ru(4)–Ru(5)	134.3	131.2	133.8	124.9

butterfly (from 152 to 166°) which is accompanied by a closing of the Ru(2)–Ru(3)–Ru(4)–Ru(5) system (from 134 to 125°). These changes in stereochemistry probably reflect a redistribution of electron density within the Ru_5 core, similar to that found in some Ru_4 complexes [5]. The effect is particularly noticeable with more electron-rich systems, which generally have larger dihedrals and longer Ru–Ru bonds.

The redistribution of electron density is also accomplished in part by the presence of semibridging and bridging carbonyl ligands. Semibridging carbonyls were found between Ru(4) and Ru(5) [Ru(5)–C(51)–O(51) 159.1(7), 161.2(9)°, **3a** and **3c**, respectively; Ru(4)–C(51) 2.549(8), 2.64(1) Å, **3a** and **3c**, respectively]. In complex **4**, an asymmetric bridging carbonyl was found between Ru(1) and Ru(5) [Ru(1)–C(52) 2.15(2) Å, Ru(5)–C(52) 2.02(2) Å]. The phosphido, phosphite and phosphino-acetylide Ru–P distances are in the ranges 2.242(2)–2.369(2) (**3a**), 2.220(2)–2.368(2) (**3c**), 2.246(7)–2.391(6) Å (**4**), with the longest values being found for the phosphines and the shortest values for the phosphite ligands. Some reorientation of the phosphino-acetylide with respect to the metal core is evident: Ru–C distances are 2.050(8)–2.323(6) (**3a**), 2.051(9)–2.240(9) (**3c**) and 2.07(1)–2.33(2) Å (**4**), the shorter bonds being Ru(2)–C(132), Ru(3)–C(132) and Ru(4)–C(131). In **1**, the Ru(4)–C(132) distance is 2.59 Å; for **3a** and **3c**, the interaction between C(132) and Ru(4) is also non-bonding [2.487(9), 2.507(8) Å, respectively], whereas in **4** the distance of 2.33(2) Å indicates a rather long Ru–C bond. The acetylide C≡C distances are 1.35(1) (**3a**), 1.33(1) (**3c**) and 1.35(2) Å (**4**), all slightly shorter than the 1.383(6) Å found for **1**.

The location of the phosphite in **3b** was established on the basis of the spectroscopic data. The Ru sites available include Ru(1), Ru(2) and Ru(5) (see below for results for **3a** and **3c**). It has also been established that nucleophilic attack of phosphine ligands can occur at the σ-carbon of μ_3-η^2-acetylide and vinylidene ligands; this may be followed by transfer of the phosphorus ligand to the metal core [6,7]. However, no evidence for the formation of complexes of this type was obtained in this work. A substantial study of mono- and bis-substituted triruthenium clusters [8] found no evidence for the presence of isomers formed through substitution at the different equatorial positions on the same metal site.

The ^{31}P NMR spectrum for complex **3b** showed that there were other isomers of this complex (with near-identical signals) present in solution. The environment for P(1) (δ 43.5) was very similar to that in **3c** (δ 43.9), although the P(2) and P(3) environments had changed substantially [δ 300.0, 134.1, respectively (**3b**); 292.5, 137.6, respectively (**3c**)], and phosphorus-phosphorus coupling was apparent (J_{av} = 34.5 Hz).

The IR ν(CO) pattern of **3b** was similar to that of **3a**, and a bridging carbonyl absorption was found at 1801 cm^{-1}. A bridging carbonyl absorption at 1791 cm^{-1} was also found for **4**, where the CO bridges the Ru(1)–Ru(5) bond. Complex **4**, which has been shown to be substituted at Ru(1) and Ru(4), was the major product obtained from the reaction of **3b** with further $P(OEt)_3$. These observations lead us to believe that in the formation of **3b**, phosphite substitution has taken place at Ru(1), with the phosphite *trans* to the phosphino-acetylide.

Discussion

This discussion necessarily supposes that the phosphite is attached to the ruthenium from which CO dissociation has occurred. While previous studies on phosphite substitution reactions of $Fe_2Os(CO)_{12}$ [9] have indicated that this is not always the case, the lack of interconversion of isomers of **3** makes this a reasonable assumption. It seems likely that all five ruthenium sites are available for CO substitution, as several other minor products were also noted in the reactions with

$P(OEt)_3$. Thermal reaction favours mono-substitution at Ru(3), a basal ruthenium, whereas the Me_3NO-promoted reaction resulted in wingtip-substitution at Ru(4). The identity of the third monosubstituted isomer **3b** can only be inferred from spectroscopic data, as this complex was not stable in solution for prolonged periods. The thermal substitution at Ru(3) suggests that the carbonyl ligands on Ru(3) are the most labile, presumably as a result of electronic and steric effects [10].

Changing the solvent polarity for the thermal reactions resulted in different proportions of the same products (see Scheme 2). Thus, in cyclohexane, the ratio of **3c** to **4** was 2/1, whereas in acetone the ratio was 1/3. Separate experiments have demonstrated that the formation of **4** does not proceed through **3c**, and that the isomers of **3** do not interconvert in solution. The disubstituted cluster **4** may be formed through further substitution of CO in either **3a** or **3b**. The addition of *P*-donor ligands to metal carbonyl clusters has been shown to accelerate the CO-substitution process in some cases [9–11]. Such acceleration may be involved in the formation of **4**, which occurred even with a 1/1 ratio of reactants. Under thermal reaction conditions similar to those used in the formation of **4** from **1**, complete reaction of isomers **3a**, **3b** and **3c** with $P(OEt)_3$ required an excess of the ligand and longer times. Without kinetic studies, it is not possible to determine whether phosphite substitution does result in acceleration of CO dissociation from **1**, or if initial multiple CO loss is involved to form a $(CO)_{11}$ intermediate.

The observed product distribution for the Me_3NO-promoted reaction suggests that different intermediate(s) are involved. As the attack of Me_3NO on cluster carbonyl ligands has been shown to occur by nucleophilic attack on the C atom of the carbonyl ligand [12], the formation of **3a** and **3b** suggests that the most electrophilic carbonyls are those on Ru(1) and Ru(4).

CO substitution by PMe_2Ph in 1

A complex formulated as $Ru_5(\mu_5\text{-}C_2PPh_2)(\mu\text{-}PPh_2)(CO)_{11}(PMe_2Ph)_2$ (**5**) was isolated from the reaction of a two-fold excess of PMe_2Ph with **1**. A reliable analysis could not be obtained for this rather unstable compound, which was characterized spectroscopically. The IR ν(CO) pattern was similar to that of **4**; the terminal bands

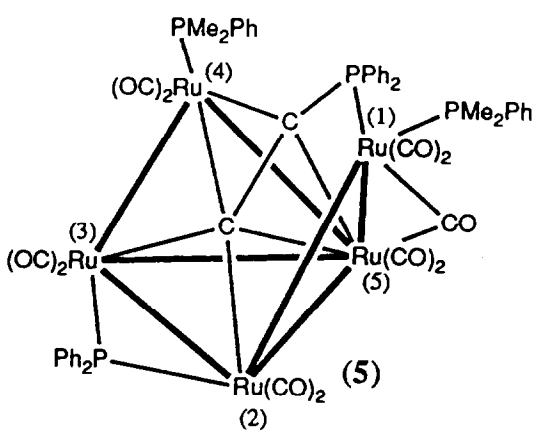

(5)

were approximately 40 cm^{-1} lower than those of **1**, and a bridging carbonyl absorption was present at 1775 cm^{-1}. It seems likely that **5** is substituted at Ru(1), since a bridging carbonyl absorption was also found for **3b** and **4**, and at Ru(4). In the FAB mass spectrum, a molecular ion was found at *m/z* 1485, which fragmented by loss of eleven CO groups. The ^1H NMR spectrum contained two signals for the Me groups at δ 1.19 and 0.93, while the phenyl resonances were between δ 7.8 and 6.5. The ^{31}P NMR spectrum showed two PMe_2Ph resonances at δ 1.5 and 23.7; the C_2PPh_2 resonance was found at δ 39.2 and the μ-PPh_2 resonance at δ 269.6. The latter two resonances were similar to those of the phosphite-substituted products.

Conclusions

Mono-substitution of CO by $P(OEt)_3$ in **1** afforded at least three isomeric products; relative amounts differ in the thermal and Me_3NO-induced reactions (Scheme 2). The most favoured sites of attack are at Ru(3) and Ru(4), respectively. The thermal reactions appear to proceed through dissociative CO loss [11b,13,14] at Ru(1), Ru(3) or Ru(4) to generate $(CO)_{12}$ intermediates, which then undergo phosphite addition to form **3a**, **3b** and **3c**. The most favoured pathway was that resulting in the formation of **3c**. A competing process involved in the thermal reactions was the substitution of two CO ligands in **1** resulting in the formation of the disubstituted complex **4**.

Experimental

General conditions

All reactions were carried out under dry nitrogen using standard Schlenk techniques. Solvents were dried and distilled before use. TLC was carried out on glass plates (20 × 20 cm) coated with silica gel (Merck 60 GF_{254}, 0.5 mm thick). Elemental analyses were by the Canadian Microanalytical Service, New Westminster, B.C., Canada V3M 1S3.

Starting materials. Complex **1** was prepared by the literature method [15]. $P(OEt)_3$ (Strem) was distilled from 4 Å molecular sieves before use. $Me_3NO \cdot 2H_2O$ (Aldrich) was dehydrated by sublimation (100 °C/0.1 mmHg).

Instruments. Perkin–Elmer 683 double beam, NaCl optics (IR); Bruker CXP300 (NMR; ^1H at 300.13 MHz, ^{31}P at 121.49 MHz); VG ZAB 2HF (FAB-MS, using 3-nitrobenzyl alcohol as matrix, exciting gas Ar, FAB gun voltage 7.5 kV, current 1 mA, accelerating potential 7 kV).

*Syntheses of three isomers of $Ru_5(\mu_5\text{-}C_2PPh_2)(\mu\text{-}PPh_2)(CO)_{12}\{P(OEt)_3\}$ (**3a**, **3b** and **3c**), and $Ru_5(\mu_5\text{-}C_2PPh_2)(\mu\text{-}PPh_2)(CO)_{11}\{P(OEt)_3\}_2$ (**4**)*

(a) Me_3NO-assisted reaction. A solution of **1** (100 mg, 0.079 mmol) in acetone (50 mL) was cooled to 0 °C and then Me_3NO (6 mg, 0.08 mmol) and $P(OEt)_3$ (16 mg, 0.096 mmol) were added in quick succession. The solution was allowed to warm to room temperature over 30 min and further portions of $P(OEt)_3$ (8 mg, 0.048 mmol) and Me_3NO (3 mg, 0.04 mmol) were added. After a further 15 min all the starting cluster had been consumed (spot TLC) and the solvent was removed under vacuum. Preparative TLC of the residue (petroleum spirit/acetone/CH_2Cl_2 14/2/1) separated nine bands of which only the major two were collected. The first brown

band (R_f 0.35) crystallized (CH_2Cl_2/petroleum spirit) as dark brown crystals of $Ru_5(\mu_5\text{-}C_2PPh_2)(\mu\text{-}PPh_2)(CO)_{12}\{P(OEt)_3\} \cdot 0.5CH_2Cl_2$ (**3a**) (39 mg, 0.028 mmol, 35%), m.p. 270 °C (dec.). Anal. Found: C, 36.96; H, 2.51; M_r 1402 (mass spectrometry). $C_{44}H_{35}O_{15}P_3Ru_5 \cdot 0.5CH_2Cl_2$ calcd.: C, 37.00; H, 2.5%; M_r 1402 (unsolvated). IR (cyclohexane): ν(CO) 2061m, 2029s, 2007(sh), 2001s, 1990(sh), 1971m, 1953w, 1933w cm^{-1}. ^1H NMR ($CDCl_3$): δ 7.9–7.3 (m, 20H, Ph); 5.30 (s, 1H, CH_2Cl_2); 3.92 (p, J(HH) = 7.0 Hz, 6H, CH_2); 1.17 (t, J(HH) = 7.0 Hz, 9H, CH_3). ^{31}P NMR (CH_2Cl_2): δ 292.9 (s, PPh_2); 140.8 (s, $P(OEt)_3$); 44.2 (s, C_2PPh_2). FAB-MS: 1402, $[M]^+$; ions formed by loss of up to 12 CO groups. A second brown band (R_f 0.38) was rechromatographed (TLC petroleum spirit/Et_2O/acetone 17/3/1). The major brown band (R_f 0.25) that developed was quickly removed from the TLC medium, precipitated (CH_2Cl_2/MeOH) by volume reduction (at −70 °C), and washed with EtOH and pentane (−70 °C). This product, an isomer of $Ru_5(\mu_5\text{-}C_2PPh_2)(\mu\text{-}PPh_2)(CO)_{12}\{P(OEt)_3\}$ (**3b**) (13 mg, 0.0093 mmol, 12%), was unstable in solution and a crystalline sample suitable for X-ray or elemental analysis could not be prepared. IR (cyclohexane): ν(CO) 2070m, 2034s, 2012s, 2002s, 1980(sh), 1953w, 1948w, 1934w, 1801w cm^{-1}. ^1H NMR ($CDCl_3$): δ 7.6–7.2 (m, 20H, Ph); 4.03 (p, J = 6.7 Hz, 6H, CH_2); 1.20 (t, J = 6.9 Hz, 9H, CH_3). ^{31}P NMR (CH_2Cl_2): δ 300.0 (s, PPh_2); 134.1 (2 × d, J = 34, 35 Hz, $P(OEt)_3$); 43.5 (m, C_2PPh_2). FAB-MS: 1402, $[M]^+$; ions formed by loss of up to 12 CO groups.

(b) Thermal reactions. (i) In cyclohexane: A solution of **1** (100 mg, 0.079 mmol) dissolved in cyclohexane (30 mL) was heated (45 °C), and $P(OEt)_3$ (24 mg, 0.145 mmol) was then added portion-wise over 45 min. Following this the solvent was removed under reduced pressure and the residue purified by TLC (petroleum spirit/acetone/CH_2Cl_2 14/2/1). Five bands were collected, the first (R_f 0.50, brown) being identified (IR, FAB-MS) as unreacted **1** (34 mg, 0.027 mmol, 34%). The second band (R_f 0.40, ochre) crystallized (CH_2Cl_2/MeOH) as dark red-brown crystalline $Ru_5(\mu_5\text{-}C_2PPh_2)(\mu\text{-}PPh_2)(CO)_{12}\{P(OEt)_3\}$ (**3c**) (25 mg, 0.017 mmol, 23%), m.p. 219–220 °C. Anal. Found: C, 37..33; H, 2.48; M_r 1402 (mass spectrometry). $C_{44}H_{35}O_{15}P_3Ru_5$ calcd.: C, 37.70; H, 2.40%; M_r 1402. IR (cyclohexane): ν(CO) 2071w, 2052s, 2005s, 1984(sh), 1971(sh), 1945w cm^{-1}. ^1H NMR ($CDCl_3$): δ 8.0–7.3 (m, 20H, Ph); 3.41 (m, 6H, CH_2); 0.96 (t, J(HH) = 7.0 Hz, 9H, CH_3). ^{31}P NMR (CH_2Cl_2): δ 292.5 (s, PPh_2); 137.6 (s, $P(OEt)_3$); 43.9 (s, C_2PPh_2). FAB-MS: 1402, $[M]^+$; ions formed by loss of up to 12 CO groups. The two middle brown bands (R_f 0.35 and 0.33) were identified (IR, FAB-MS) as **3b** (4 mg, 0.003 mmol, 4%), and **3a** (6 mg, 0.004 mmol, 5%). The last band (R_f 0.28, brown) was crystallized (CH_2Cl_2/petroleum spirit) by slow evaporation and cooling to give dark brown crystals of $Ru_5(\mu_5\text{-}C_2PPh_2)(\mu\text{-}PPh_2)(CO)_{11}\{P(OEt)_3\}_2$ (**4**) (14 mg, 0.0091 mmol, 11%), m.p. 213–214 °C. Anal. Found: C, 38.01; H, 3.19; M_r 1540 (mass spectrometry, $[M + 2H]^+ = 1542$). $C_{49}H_{50}O_{17}P_4Ru_5$ calcd.: C, 38.21; H, 3.27%; M_r 1540. IR (cyclohexane): ν(CO) 2038m, 2018s, 1992s, 1983(sh), 1965m, 1943m, 1926(sh), 1791w cm^{-1}. ^1H NMR ($CDCl_3$): δ 8.1–7.3 (m, 20H, Ph); 3.92 (m, 6H, CH_2); 3.77 (p, J = 7.0 Hz, 6H, CH_2); 1.18 (t, J(HH) = 7.0 Hz, 9H, CH_3); 1.11 (t, J(HH) = 7.0 Hz, 9H, CH_3). ^{31}P NMR (CH_2Cl_2): δ 277.3 (s, PPh_2); 142.8 (s, $P(OEt)_3$); 137.1 (d, J = 40 Hz, $P(OEt)_3$); 44.8 (d, J = 40 Hz, C_2PPh_2). FAB-MS: 1542. $[M]^+$; ions formed by loss of up to 9 CO groups. Three other minor/trace bands were not characterized further. No conversion between the three isomers of **3** was detected by ^1H or ^{31}P NMR ($CDCl_3$ or CH_2Cl_2, 2 h, r.t.).

Table 2

Fractional atomic coordinates for $Ru_5(\mu_5\text{-}C_2PPh_2)(\mu\text{-}PPh_2)(CO)_{12}\{P(OEt)_3\}$ (3a)

Atom	x	y	z
Ru(1)	0.35509(3)	0.57395(6)	1.02833(7)
Ru(2)	0.23357(3)	0.59114(6)	1.13052(7)
Ru(3)	0.16041(3)	0.43120(6)	1.10888(7)
Ru(4)	0.24490(3)	0.23054(6)	1.08054(7)
Ru(5)	0.26219(3)	0.47980(6)	0.92545(7)
C(11)	0.4261(4)	0.5687(8)	0.9248(9)
O(11)	0.4669(3)	0.5735(7)	0.8570(8)
C(12)	0.3297(4)	0.7408(9)	0.893(1)
O(12)	0.3197(4)	0.8393(7)	0.8093(8)
C(13)	0.3817(4)	0.6212(9)	1.170(1)
O(13)	0.3994(4)	0.6558(8)	1.2514(8)
C(21)	0.2554(4)	0.5796(9)	1.312(1)
O(21)	0.2696(4)	0.5688(8)	1.4249(7)
C(22)	0.2321(4)	0.7649(9)	1.065(1)
O(22)	0.2302(4)	0.8701(6)	1.0259(9)
C(31)	0.1229(4)	0.3302(8)	1.266(1)
O(31)	0.0979(3)	0.2688(6)	1.3598(8)
C(32)	0.0992(4)	0.4235(8)	0.993(1)
O(32)	0.0627(3)	0.4194(7)	0.9145(8)
C(41)	0.1773(4)	0.1862(9)	1.013(1)
O(41)	0.1379(4)	0.1592(7)	0.9670(8)
C(42)	0.3034(4)	0.1316(8)	1.022(1)
O(42)	0.3379(3)	0.0715(7)	0.9823(8)
C(51)	0.2276(4)	0.3973(9)	0.828(1)
O(51)	0.2060(4)	0.3809(7)	0.7323(7)
C(52)	0.3276(4)	0.4993(9)	0.8010(9)
O(52)	0.3599(3)	0.5152(7)	0.7075(7)
C(53)	0.2188(5)	0.6384(9)	0.817(1)
O(53)	0.1947(4)	0.7341(7)	0.7370(8)
P(1)	0.3719(1)	0.3601(2)	1.1791(2)
C(111)	0.4314(4)	0.2488(8)	1.1515(9)
C(112)	0.4514(4)	0.2658(9)	1.016(1)
C(113)	0.4978(5)	0.183(1)	0.998(1)
C(114)	0.5249(5)	0.083(1)	1.110(1)
C(115)	0.5063(6)	0.064(1)	1.243(1)
C(116)	0.4597(5)	0.145(1)	1.264(1)
C(121)	0.3811(4)	0.3221(8)	1.3699(8)
C(122)	0.4324(5)	0.346(1)	1.424(1)
C(123)	0.4408(5)	0.316(1)	1.569(1)
C(124)	0.3992(5)	0.260(1)	1.664(1)
C(125)	0.3488(5)	0.239(1)	1.609(1)
C(126)	0.3391(5)	0.265(1)	1.465(1)
C(131)	0.3007(4)	0.3278(7)	1.1447(8)
C(132)	0.2517(4)	0.4048(6)	1.1565(7)
P(2)	0.1272(1)	0.6185(2)	1.1189(3)
C(211)	0.0871(4)	0.7539(7)	0.9701(9)
C(212)	0.0828(5)	0.8704(8)	0.969(1)
C(213)	0.0553(5)	0.9731(9)	0.856(1)
C(214)	0.0301(5)	0.958(1)	0.744(1)
C(215)	0.0319(6)	0.843(1)	0.743(1)
C(216)	0.0608(5)	0.7402(9)	0.857(1)
C(221)	0.0853(4)	0.6224(7)	1.2744(9)
C(222)	0.0276(4)	0.6872(8)	1.263(1)

Table 2 (continued)

Atom	x	y	z
C(223)	−0.0010(4)	0.6863(9)	1.388(1)
C(224)	0.0275(5)	0.6196(9)	1.518(1)
C(225)	0.0836(5)	0.5540(9)	1.532(1)
C(226)	0.1123(4)	0.5531(9)	1.411(1)
P(4)	0.2484(1)	0.0761(2)	1.2972(3)
O(411)	0.2261(3)	0.1242(5)	1.4162(6)
C(411)	0.2303(7)	0.048(1)	1.567(1)
C(412)	0.1947(7)	0.111(1)	1.645(1)
O(421)	0.2154(4)	−0.0351(7)	1.3145(9)
C(421)	0.1542(9)	−0.038(2)	1.325(2)
C(422)	0.1347(9)	−0.144(1)	1.384(2)
O(431)	0.3149(3)	0.0027(6)	1.3581(8)
C(431)	0.3410(9)	−0.107(2)	1.376(3)
C(432)	0.3878(8)	−0.165(2)	1.473(2)

(ii) In acetone: To **1** (200 mg, 0.16 mmol) in acetone (40 mL) was added $P(OEt)_3$ (46 mg, 0.28 mmol) over 1 h at room temperature. After a further 20 min the solvent was removed under vacuum. Preparative TLC of the residue (petroleum spirit/acetone/CH_2Cl_2 14/2/1) eluted eleven bands, of which five were collected and identified spectroscopically (IR, FAB-MS) as: (1) R_f 0.85, brown, **1** (23 mg, 0.018 mmol, 11%); (2) R_f 0.78, ochre, **3c** (22 mg, 0.016 mmol, 10%); (3) R_f 0.68, brown, **3a** (5 mg, 0.004 mmmol, 2%); (4) R_f 0.60, brown, **4** (75 mg, 0.049 mmol, 30%); and (5) R_f 0.50, orange, $Ru_5(\mu\text{-}C_2PPh_2)(\mu\text{-}PPh_2)(CO)_{14}\{P(OEt)_3\}$ (4 mg, 0.003 mmol, 2%). IR (cyclohexane): ν(CO) 2048 m, 2042(sh), 2031s, 2011w, 1996s, 1977w, 1956w, 1945w cm^{-1}. FAB-MS: 1457, $[M]^+$; ions formed by loss of up to 14 CO groups.

*(c) Attempted formation of **4** from **3a**, **3b** or **3c**.* (i) From **3a**: A solution of **3a** (7 mg, 0.005 mmol) in acetone (40 mL) was treated with $P(OEt)_3$ (12 mg, 0.072 mmol) at 33°C. After 16 h the solvent was removed under reduced pressure and the residue purified by TLC (petroleum spirit/CH_2Cl_2/acetone 7/2/1) to give a major brown band identified as **4** (IR, FAB-MS).

(ii) From **3b**: A solution of **3b** (9 mg, 0.006 mmol) in acetone (40 mL) was treated with $P(OEt)_3$ (12 mg, 0.072 mmol) at 33°C. After 16 h the solvent was removed under reduced pressure and the residue purified by TLC (petroleum spirit/CH_2Cl_2/acetone 7/2/1) to give a major brown band (R_f 0.32) that was identified as **4** (IR, FAB-MS).

(iii) From **3c**: A solution of **3c** (15 mg, 0.0011 mmol) in acetone (15 mL) was treated portionwise with $P(OEt)_3$ (11 mg, 0.066 mmol) at 45°C. After 1 h 15 min the solvent was removed under reduced pressure and the residue purified by TLC (petroleum spirit/CH_2Cl_2/acetone 14/2/1) to give four brown bands. Two bands (R_f 0.26, 0.20) were identified (FAB-MS, IR) as isomers of $Ru_5(\mu\text{-}C_2PPh_2)(\mu\text{-}PPh_2)(CO)_{11}\{P(OEt)_3\}_2$ ($[M]^+$ 1542, IR significantly different from that of **4**) and the fourth (R_f 0.37) as unreacted **3c**.

Synthesis of $Ru_5(\mu_5\text{-}C_2PPh_2)(\mu\text{-}PPh_2)(CO)_{11}(PMe_2Ph)_2$ (5)

An immediate reaction occurred when PMe_2Ph (11 mg, 0.080 mmol) was added to a solution of **1** (50 mg, 0.040 mmol) in acetone (20 mL). After 30 min the solvent

Table 3

Fractional atomic coordinates for $Ru_5(\mu_5\text{-}C_2PPh_2)(\mu\text{-}PPh_2)(CO)_{12}\{P(OEt)_3\}$ (3c)

Atom	x	y	z
Ru(1)	−0.21420(6)	0.26381(4)	0.72039(7)
Ru(2)	0.02108(6)	0.32670(3)	0.86852(6)
Ru(3)	0.23650(5)	0.25554(3)	0.88105(6)
Ru(4)	0.16557(5)	0.11746(3)	0.78478(6)
Ru(5)	0.00222(6)	0.22289(3)	0.65922(6)
P(1)	−0.1359(2)	0.1643(1)	0.8182(2)
P(2)	0.2119(2)	0.3706(1)	0.9053(2)
P(3)	0.3753(2)	0.2363(1)	1.0710(2)
C(131)	0.0116(7)	0.1655(4)	0.8127(7)
C(132)	0.0696(7)	0.2234(4)	0.8620(7)
O(311)	0.4469(6)	0.1643(3)	1.0652(7)
O(321)	0.4812(7)	0.2875(4)	1.1490(8)
O(331)	0.3330(11)	0.2414(7)	1.1817(10)
C(311)	0.5456(13)	0.1401(7)	1.1721(15)
C(312)	0.6038(14)	0.0798(7)	1.1344(17)
C(321)	0.5618(13)	0.3068(9)	1.1061(16)
C(322)	0.6711(13)	0.3420(9)	1.2208(19)
C(331)	0.2491(19)	0.2189(11)	1.2026(19)
C(332)	0.2453(22)	0.2515(12)	1.3258(17)
C(11)	−0.2631(10)	0.3377(6)	0.6167(11)
O(11)	−0.2987(9)	0.3776(5)	0.5514(10)
C(12)	−0.3581(10)	0.2152(6)	0.6046(10)
O(12)	−0.4469(8)	0.1882(5)	0.5430(10)
C(13)	−0.2743(9)	0.3112(6)	0.8376(11)
O(13)	−0.3152(9)	0.3415(5)	0.9063(10)
C(21)	−0.0591(9)	0.4102(6)	0.8186(13)
O(21)	−0.1040(9)	0.4619(5)	0.7889(13)
C(22)	−0.0001(10)	0.3484(6)	1.0168(12)
O(22)	−0.0108(9)	0.3622(5)	1.1125(9)
C(31)	0.3670(9)	0.2467(5)	0.8265(9)
O(31)	0.4431(8)	0.2416(5)	0.7907(8)
C(41)	0.2242(9)	0.0777(5)	0.9342(9)
O(41)	0.2564(8)	0.0506(4)	1.0216(7)
C(42)	0.1061(8)	0.0333(5)	0.6824(9)
O(42)	0.0823(7)	−0.0190(4)	0.6265(7)
C(43)	0.3247(10)	0.1038(5)	0.7697(10)
O(43)	0.4172(7)	0.0913(4)	0.7642(9)
C(51)	0.1274(9)	0.1862(6)	0.5965(9)
O(51)	0.1848(7)	0.1772(5)	0.5376(7)
C(52)	−0.0185(9)	0.3046(6)	0.5870(10)
O(52)	−0.0347(8)	0.3504(4)	0.5328(8)
C(53)	−0.1355(8)	0.1838(5)	0.5179(9)
O(53)	−0.2116(7)	0.1627(4)	0.4260(7)
C(111)	−0.2122(5)	0.0860(3)	0.7320(5)
C(112)	−0.1876(5)	0.0518(3)	0.6299(5)
C(113)	−0.2512(5)	−0.0064(3)	0.5602(5)
C(114)	−0.3394(5)	−0.0305(3)	0.5927(5)
C(115)	−0.3640(5)	0.0037(3)	0.6948(5)
C(116)	−0.3004(5)	0.0619(3)	0.7645(5)
C(121)	−0.1017(6)	0.1542(3)	0.9817(5)
C(122)	−0.0345(6)	0.0957(3)	1.0279(5)
C(123)	−0.0003(6)	0.0876(3)	1.1544(5)
C(124)	−0.0333(6)	0.1378(3)	1.2346(5)

Table 3 (continued)

Atom	x	y	z
C(125)	−0.1005(6)	0.1962(3)	1.1884(5)
C(126)	−0.1347(6)	0.2044(3)	1.0620(5)
C(211)	0.2981(6)	0.4239(3)	1.0530(6)
C(212)	0.2893(6)	0.4128(3)	1.1641(6)
C(213)	0.3613(6)	0.4494(3)	1.2798(6)
C(214)	0.4421(6)	0.4971(3)	1.2844(6)
C(215)	0.4509(6)	0.5081(3)	1.1733(6)
C(216)	0.3788(6)	0.4715(3)	1.0577(6)
C(221)	0.2083(7)	0.4195(3)	0.7835(6)
C(222)	0.1548(7)	0.4852(3)	0.7801(6)
C(223)	0.1404(7)	0.5211(3)	0.6817(6)
C(224)	0.1795(7)	0.4913(3)	0.5866(6)
C(225)	0.2330(7)	0.4256(3)	0.5900(6)
C(226)	0.2474(7)	0.3897(3)	0.6884(6)

was removed under vacuum and the products separated by TLC (petroleum spirit/CH_2Cl_2 4/3). A major brown band (R_f 0.30) was separated from the four other minor bands and crystallized (CH_2Cl_2/MeOH) as brown plates of $Ru_5(\mu_5\text{-}C_2PPh_2)(\mu\text{-}PPh_2)(CO)_{11}(PMe_2Ph)_2$ (**5**) (43 mg, 0.029 mmol, 72%), m.p. 241–243°C. Reproducible analyses could not be obtained for this complex. IR (cyclohexane): ν(CO) 2038(sh), 2034m, 2014s, 1988vs, 1962w, 1953w, 1933m, 1775w cm^{-1}. ^1H NMR (C_6D_6): δ 7.8–6.5 (m, 30H, Ph); 1.19 (d, J(PH) = 10.0 Hz, 6H, Me); 0.93 (d, J(PH) = 10.5 Hz, 6H, Me). ^{31}P NMR (CH_2Cl_2): δ 269.6 (s, PPh_2); 39.2 (s, C_2PPh_2); 23.7, 1.5 (2 × s, PMe_2Ph). FAB-MS: 1485, $[M]^+$; ions formed by loss of up to 11 CO groups.

Crystallography

Intensity data for **3a** and **3c** were measured at room temperature on an Enraf-Nonius CAD4F diffractometer fitted with Mo-K_α (graphite monochromatised) radiation, $\lambda = 0.71073$ Å. Data for **4** were measured at 138 K on a Nicolet $P3$ diffractometer using monochromatised Mo-K_α radiation, $\lambda = 0.71069$ Å. Data collection parameters and unit cell dimensions are listed in Table 5. The $h\,k\,l$ ranges for **3a** and **3c** were $\pm h$, $\pm k$, $+l$ and $+h$, $\pm k$, $\pm l$, respectively. For **4** experimental difficulties precluded the measurement of all the data. Whereas data for k and l were measured up to θ 22.5°, those for h were limited to $\theta < 15°$ owing to irretrievable loss of the crystal due to icing problems. For **3c** there was a 5% decrease in the net intensities of three standard reflections measured after every 3600 s X-ray exposure time; the data were corrected for this variation assuming a linear deterioration. The data sets were corrected routinely for Lorentz and polarisation effects and for absorption. A Gaussian procedure was used for **3a** such that $A^*_{min,max}$ were 1.06 and 1.25, respectively. An analytical procedure was employed for **3c** such that the max/min transmission factors were 0.804 and 0.723, respectively, and a ϕ scan technique was employed for **4** with max and min transmission factors being 0.97 and 0.59, respectively.

All three structures were solved by direct methods. Blocked-matrix least-squares refinement was employed for **3a** and **3c** and a full-matrix least-squares procedure

Table 4

Fractional atomic coordinates for $Ru_5(\mu_5\text{-}C_2PPh_2)(\mu\text{-}PPh_2)(CO)_{11}\{P(OEt)_3\}_2$ (4)

Atom	x	y	z
Ru(1)	0.4421(2)	0.2270(1)	0.2459(1)
Ru(2)	0.5996(2)	0.1429(1)	0.3165(1)
Ru(3)	0.6365(2)	0.0307(1)	0.2625(1)
Ru(4)	0.6203(2)	0.0610(1)	0.1326(1)
Ru(5)	0.4523(2)	0.1043(1)	0.2140(1)
P(1)	0.5903(6)	0.2216(2)	0.1707(1)
P(2)	0.7032(6)	0.0652(1)	0.3560(1)
P(3)	0.3548(6)	0.3052(2)	0.1981(2)
P(4)	0.8021(6)	0.0548(2)	0.0988(2)
C(131)	0.613(2)	0.1447(5)	0.1696(5)
C(132)	0.643(2)	0.1166(6)	0.2237(5)
C(11)	0.528(2)	0.2756(6)	0.3026(5)
O(11)	0.571(1)	0.3084(4)	0.3382(4)
C(12)	0.322(2)	0.2193(6)	0.3051(7)
O(12)	0.247(2)	0.2165(5)	0.3376(5)
C(21)	0.714(2)	0.1963(6)	0.3441(6)
O(21)	0.788(1)	0.2275(5)	0.3600(4)
C(22)	0.508(2)	0.1578(6)	0.3840(6)
O(22)	0.444(1)	0.1674(4)	0.4258(4)
C(31)	0.760(2)	−0.0182(6)	0.2482(6)
O(31)	0.842(1)	−0.0491(5)	0.2432(4)
C(32)	0.545(2)	−0.0270(6)	0.2974(6)
O(32)	0.486(1)	−0.0630(4)	0.3173(4)
C(41)	0.566(2)	0.0713(6)	0.0499(6)
O(41)	0.530(1)	0.0765(4)	−0.0016(4)
C(42)	0.606(2)	−0.0231(6)	0.1341(5)
O(42)	0.596(1)	−0.0729(4)	0.1302(4)
C(51)	0.384(2)	0.0618(5)	0.1452(5)
O(51)	0.330(1)	0.0382(4)	0.1079(4)
C(52)	0.333(2)	0.1668(7)	0.1931(7)
O(52)	0.240(2)	0.1690(5)	0.1681(5)
C(53)	0.359(2)	0.0641(6)	0.2695(6)
O(53)	0.299(1)	0.0370(4)	0.3006(4)
O(311)	0.285(1)	0.2921(4)	0.1347(4)
C(311)	0.180(2)	0.3183(8)	0.1093(8)
C(312)	0.128(2)	0.2796(8)	0.0590(8)
O(321)	0.449(1)	0.3541(4)	0.1839(4)
C(321)	0.418(2)	0.4106(6)	0.1539(6)
C(322)	0.460(2)	0.4084(6)	0.0868(6)
O(331)	0.257(1)	0.3391(4)	0.2355(4)
C(331)	0.290(2)	0.3697(6)	0.2925(6)
C(332)	0.185(2)	0.3965(8)	0.3196(8)
O(411)	0.835(1)	0.0904(4)	0.0368(4)
C(411)	0.816(2)	0.1531(6)	0.0307(7)
C(412)	0.836(2)	0.1738(8)	−0.0304(7)
O(421)	0.849(1)	−0.0068(4)	0.0789(4)
C(421)	0.805(2)	−0.0355(6)	0.0223(6)
C(422)	0.833(2)	−0.0989(6)	0.0243(6)
O(431)	0.898(2)	0.0731(4)	0.1513(4)
C(431)	1.021(3)	0.0679(6)	0.1416(7)
C(432)	1.068(2)	0.0154(7)	0.1759(7)
C(111)	0.6417(9)	0.2784(4)	0.0573(4)
C(112)	0.6227(9)	0.2904(4)	−0.0065(4)

Table 4 (continued)

Atom	x	y	z
C(113)	0.5264(9)	0.2667(4)	−0.0390(4)
C(114)	0.4492(9)	0.2310(4)	−0.0079(4)
C(115)	0.4681(9)	0.2190(4)	0.0558(4)
C(116)	0.5644(9)	0.2427(4)	0.0884(4)
C(121)	0.740(1)	0.3102(4)	0.2158(4)
C(122)	0.847(1)	0.3335(4)	0.2358(4)
C(123)	0.947(1)	0.2996(4)	0.2333(4)
C(124)	0.941(1)	0.2423(4)	0.2109(4)
C(125)	0.834(1)	0.2190(4)	0.1910(4)
C(126)	0.733(1)	0.2529(4)	0.1934(4)
C(211)	0.647(1)	0.0579(3)	0.4816(3)
C(212)	0.630(1)	0.0289(3)	0.5381(3)
C(213)	0.641(1)	−0.0318(3)	0.5413(3)
C(214)	0.669(1)	−0.0635(3)	0.4879(3)
C(215)	0.685(1)	−0.0345(3)	0.4314(3)
C(216)	0.674(1)	0.0262(3)	0.4282(3)
C(221)	0.922(1)	0.0608(4)	0.4194(3)
C(222)	1.041(1)	0.0716(4)	0.4253(3)
C(223)	1.099(1)	0.0966(4)	0.3757(3)
C(224)	1.038(1)	0.1107(4)	0.3200(3)
C(225)	0.919(1)	0.0999(4)	0.3141(3)
C(226)	0.861(1)	0.0749(4)	0.3637(3)

Table 5

Crystal data and refinement details for **3a**, **3c** and **4**

	3a	**3c**	**4**
Formula	$C_{44}H_{35}O_{15}P_3Ru_5$	$C_{44}H_{35}O_{15}P_3Ru_5$	$C_{49}H_{50}O_{17}P_4Ru_5$
MW	1402.0	1402.0	1540.2
Crystal system	triclinic	triclinic	monoclinic
Space group	$P\bar{1}$	$P\bar{1}$	$P2_1/n$
a, Å	22.343(6)	11.821(3)	11.521(8)
b, Å	11.830(3)	19.958(5)	22.863(32)
c, Å	10.132(4)	11.670(2)	21.323(15)
α, deg	67.28(2)	99.41(3)	90
β, deg	89.21(3)	114.14(2)	92.21(6)
γ, deg	81.15(2)	84.12(3)	90
U, Å^3	2438	2477	5612
Z	2	2	4
D_c, g cm^{-3}	1.910	1.879	1.823
$F(000)$	1368	1368	3040
Crystal size, mm	0.05×0.17×0.24	0.18×0.18×0.50	0.26×0.16×0.08
μ, cm^{-1}	15.1	15.9	14.0
θ limits, deg	1.5–25.0	1.5–22.5	< 22.5 (see text)
Scan technique	$\theta/2\theta$	$\omega:2/3\theta$	Wycoff scans
No. data collected	8321	7096	7127
No. unique data	8321	6484	4156
Criterion obs.	$I \geq 3.0\sigma(I)$	$I \geq 2.5\sigma(I)$	$I \geq 3.0\sigma(I)$
No. data used	5260	4265	3032
g	0.003	0.003	0.0005
R	0.042	0.042	0.050
R_w	0.040	0.044	0.048

was used for the refinement of **4**. For **3a** all non-H atoms were refined anisotropically whereas for **3c** only non-H, non-phenyl atoms were refined anisotropically. In **4** only the five Ru atoms were refined anisotropically. In the refinements of **3c** and **4**, phenyl groups were treated as hexagonal rigid groups. Hydrogen atoms were included in each model at their calculated positions. For **3a** statistical weights derived from the expression $\sigma^2(I) = [\sigma^2(I_{\text{diff}}) + 0.0004\sigma^4(I_{\text{diff}})]$ were used. For the refinements of **3c** and **4** a weighting scheme of the form $w = [\sigma^2(F) + g|F|^2]^{-1}$ was applied.

Calculations for **3a** were performed with the XTAL 2.4 programme system implemented by Hall [16]. The SHELX-76 system [17] was employed for the solution and refinement of the **3c** structure whereas for **4** the SHELXS-86 programme [18] was used. Neutral atom scattering factors (with corrections applied for f' and f'') were from ref. 19. Fractional atomic coordinates for the three compounds are given in Tables 2–4 and the numbering schemes employed are shown in Figs. 1–3 which were drawn with PLUTO [20]. Supplementary material comprises thermal parameters, hydrogen atom parameters, all bond distances and angles and the observed and calculated structure factors, and is available upon request from one of the authors (ERTT).

Acknowledgements

We thank the Australian Research Council for support of this work. MJL acknowledges the receipt of a Commonwealth Post-graduate Research Award.

References

1 Part LXVII: M.I. Bruce, G.A. Koutsantonis and E.R.T. Tiekink, J. Organomet. Chem., 408 (1991) 77.
2 M.I. Bruce, M.L. Williams, J.M. Patrick and A.H. White, J. Chem. Soc., Dalton Trans., (1985) 1229.
3 M.I. Bruce, M.L. Williams, B.W. Skelton and A.H. White, J. Organomet. Chem., 369 (1989) 393.
4 R.K. Harris, Can. J. Chem., 42 (1964) 2275.
5 A.J. Carty, S.A. MacLaughlin, J. van Wagner and N.J. Taylor, Organometallics, 1 (1982) 1013.
6 T. Albiez and H. Vahrenkamp, Angew. Chem., 99 (1987) 561; Angew. Chem., Int. Ed. Engl., 26 (1987) 572.
7 M.I. Bruce, G.A. Koutsantonis and E.R.T. Tiekink, J. Organomet. Chem., 407 (1991) 391.
8 M.I. Bruce, M.J. Liddell, C.A. Hughes, B.W. Skelton and A.H. White, J. Organomet. Chem., 347 (1988) 157; M.I. Bruce, M.J. Liddell, J.M. Patrick, B.W. Skelton and A.H. White, ibid., 347 (1988) 181; M.I. Bruce, M.J. Liddell, O. bin Shawkataly, C.A. Hughes, B.W. Skelton and A.H. White, ibid., 347 (1988) 207; M.I. Bruce, M.J. Liddell, O. bin Shawkataly, I.R. Bytheway, B.W. Skelton and A.H. White, ibid., 369 (1989) 217.
9 R. Shojaie and J.D. Atwood, Inorg. Chem., 27 (1988) 2558.
10 (a) D.J. Darensbourg and B.J. Baldwin-Zuschke, J. Am. Chem. Soc., 104 (1982) 3906; (b) D.C. Sonnenberger and J.D. Atwood, ibid., 104 (1982) 2113.
11 (a) R. Ros, A. Scrivanti, V.G. Albano, D. Braga and L. Garlaschelli, J. Chem. Soc., Dalton Trans., (1986) 2411; (b) B.F.G. Johnson, Inorg. Chim. Acta, 115 (1986) L39; (c) K.J. Karel and J.R. Norton, J. Am. Chem. Soc., 96 (1974) 6812; (d) S.K. Malik and A.J. Poë, Inorg. Chem., 17 (1978) 1484.
12 J.K. Shen, Q.Z. Shi, and F. Basolo, Inorg. Chem., 27 (1988) 4236; J.K. Shen, Y.L. Shi, Y.C. Gao, Q.Z. Shi and F. Basolo, J. Am. Chem. Soc., 110 (1988) 2414.
13 R. Shojaie and J.D. Atwood, Inorg. Chem., 26 (1987) 2199.
14 J.P. Candlin and A.C. Shortland, J. Organomet. Chem., 16 (1969) 289.
15 M.I. Bruce, M.J. Liddell and E.R.T. Tiekink, J. Organomet. Chem., 391 (1990) 81.
16 J.M. Stewart and S.R. Hall (Eds.), The XTAL System of Crystallographic Programmes: Users' Manual. Technical Report TR-901, Computer Science Center, University of Maryland, Maryland, USA, 1983.

17 G.M. Sheldrick, SHELX-76, Programme for crystal structure determination, University of Cambridge, England, 1976.
18 G.M. Sheldrick, SHELXS-86, Programme for the automatic solution of crystal structures, University of Göttingen, Germany, 1986.
19 J.A. Ibers and W.C. Hamilton (Eds.), International Tables for X-ray Crystallography, Vol. IV, The Kynoch Press, Birmingham, England, 1974.
20 W.D.S. Motherwell, PLUTO, Plotting programme for molecular structures, University of Cambridge, England, 1978.